Flow around Wing Sections with High-Lift Devices

D. N. FOSTER*
Royal Aircraft Establishment, Farnborough, Hampshire, England.

A combined theoretical and experimental study has been made of the two-dimensional flow around a wing with a slat and slotted flap. Detailed measurements of the surface pressures and of the characteristics of the viscous layer were obtained, while special care was taken to ensure that conditions were as close as possible to two-dimensional flow. Comparisons have been made with values calculated for inviscid flow, to show how the theoretical effect of variation of the position of the slat and flap was modified by viscous effects. These have allowed the flow for the position of the slat or flap which gives optimum aerodynamic performance to be described, and consideration has been given to the calculation methods required to predict this position, and the corresponding flow. Finally, some suggestions have been made as to how the characteristics of the slat and flap are likely to be affected by changes of Reynolds number, and how this work might be extended to the three-dimensional flow on a sweptback wing.

Nomenclature

c_0 = chord of wing section with high-lift devices retracted
C_f = skin-friction coefficient
C_L = lift coefficient
$C_{L\,max}$ = maximum value of the lift coefficient
V = local flow velocity
V^* = velocity corresponding to freestream total head and local static pressure
x_F = distance measured parallel to chord of flap, from origin of flap coordinates
x_W = distance measured parallel to chord of wing, from origin of wing coordinates
z_B = distance measured normal to surface of aerofoil
δ^* = displacement thickness of viscous layer
θ = momentum thickness of viscous layer

Introduction

THE high-lift devices to be considered in this paper, the slat and slotted flap, have been used on aircraft for a number of years. Data on their lift and drag increments, and on the geometric positions for optimum aerodynamic performance, have been collected on a number of occasions,[1,2] and these can provide general guidelines for new designs. No indication is given, however, of the shape of the flap or slatted leading edge which would give the best aerodynamic performance. As current designs of swept-winged aircraft demand high-lift systems of high effectiveness, lengthy tests are necessary to produce a configuration of wing and high-lift devices which yields the optimum performance. These tests may involve not only the wind tunnel but also very expensive flight tests.

In order to reduce the time and cost of the tests, and to produce designs tailored for flight Reynolds number, it is necessary to understand the nature of the flow around the wing with its high-lift devices. Interest centers on the swept-wing class of aircraft and, fortunately, variable geometry military aircraft have wing planforms in their low-speed configurations similar to those of civil aircraft. Thus the class can be considered to cover aspect ratios of, say, 6 to 9, and angles of sweepback from 20° to 40°. Although for these wings sweepback has a pronounced effect on the flow near the root and tip, both linearized theory and experiments in viscous flow would suggest that there is at least part of the wing for which the flow is similar to that in two-dimensional flow. Thus in a general investigation aimed at understanding the flow over a swept-wing with high-lift devices it should be possible to obtain meaningful results in two-dimensional flow. Subsequently, the concepts so derived can be examined on a swept wing to ascertain the limits of the validity of this approach.

Basis of Theoretical and Experimental Approach

The real flow around a wing with high-lift devices is the result of interactions between the adjacent lifting surfaces, and of interactions between the viscous flows around these surfaces. A particular feature of the flow is that the downstream components of the multiple aerofoil are in close proximity to the wakes shed from the upstream components. Although the two sets of interactions are not independent, it was considered that some insight into the flow might be gained if one of the interactions was calculated in the absence of the other.

The interaction most easily calculated is that between the adjacent lifting surfaces in potential flow, and an examination was made[3] of existing methods for calculating the pressure distribution around multiple aerofoils. At the time of this investigation (1966), exact test cases were available only for single aerofoils. On the basis of comparisons of calculated pressure distributions with exact solutions, for a range of cambered aerofoils, the method of A. M. O. Smith,[4] using surface distributions of sources, was selected.

If meaningful comparisons are to be made between the results of calculations for two-dimensional flow, and experi-

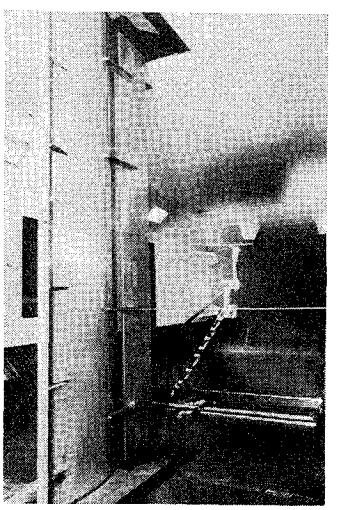

Fig. 1 The model in the wind tunnel.

Presented as Paper 71-96 at the AIAA 9th Aerospace Sciences Meeting, New York, January 25–27, 1971; submitted April 16, 1971; revision received December 18, 1971.

Index category: Airplane and Component Aerodynamics.

* Principal Scientific Officer, Aerodynamics Department.

Table 1 Number of pressure tappings on components of aerofoil section

Component		Number of pressure tappings
Slat		25
Main wing	Plain nose	62
	Drooped nose	64
	Slatted nose	55
Flap		34

mental measurements, the experimental conditions must be as close to two-dimensional flow as possible. Even with a model wing of large span, mounted between the roof and floor of the wind tunnel, Fig. 1, separation of the boundary layer on the floor and roof at the junction with the wing can result in a large variation of the chordwise loading across the span of the wing. To avoid the possibility of this separation occurring, a portion of the tunnel boundary layer was removed by suction through a perforated area of the floor and roof along the length of the junction. Previous tests[5] had shown this to be effective in reducing the spanwise variation of loading to a very small value.

Description of Model and Test Program

The model wing (Fig. 1) had a basic chord length (without extension due to high-lift devices) of 3 ft, and spanned the 9 ft dimension of the 13 ft × 9 ft low-speed wind tunnel at RAE Bedford. The wing section was of 14% thickness-chord ratio, and the model could be fitted with a 17% chord slat and 40% chord slotted flap. The wind speed for the tests was 200 ft/sec, giving a Reynolds number of 3.8×10^6, based on the unextended chord.

No direct measurements of forces were possible; the values of the lift and pitching moment coefficients were derived by integration of the surface pressures measured at the center-line of the model, and of the drag coefficient from measurements taken by a wake-survey rake. The number of pressure tappings on each component was as shown in Table 1.

The configurations of the aerofoil which have been tested are shown in Fig. 2. Preliminary tests were made for all three configurations to establish the effect on the maximum lift coefficient of varying the position of the flap relative to the wing. Similar measurements for the effect of the position of the slat were made for the third configuration. These established that movement of the flap normal to the wing chord-line, and of the slat along a line normal to the wing profile, produced the largest variation of the maximum lift coefficient. More detailed studies were then made, in which

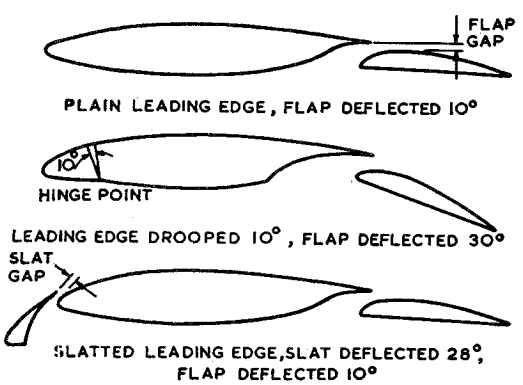

Fig. 2 Aerofoil configurations tested.

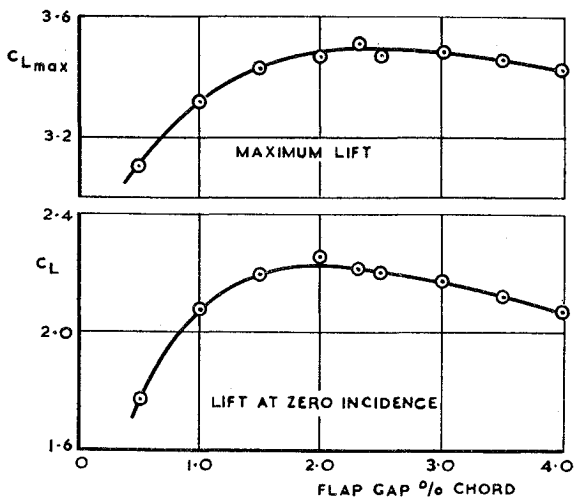

Fig. 3 Experimental effect of flap gap. Flap deflection 30°, drooped leading edge.

measurements were taken of the surface pressures and of the velocity distributions through the viscous layers, of the effect of changes of the flap gap (defined as the distance between the flap upper surface and the wing trailing edge, measured normal to the wing chord-line†) and of the slat gap (defined as the distance between the slat trailing edge and the wing surface, measured normal to the wing profile) as shown in Fig. 2.

Flow around the Wing and Flap

For all the configurations shown in Fig. 2, the increase of lift with angle of incidence was terminated by a breakdown of the flow over the main wing. Although the manner of this breakdown was dependent on the leading-edge configuration, the mechanism of the wing stall was not affected by the size of the flap gap for any leading-edge configuration.

Figures 3 and 4 show values of the maximum lift coefficient, and the lift coefficient at constant angle of incidence, for a range of values of the flap gap. Curves very similar to those shown on Fig. 4 were obtained for the plain leading edge, with the flap deflected 10°. The similarity of the shape of the two curves shown on each figure suggests that an analysis of the flow at a constant angle of incidence could lead to an understanding of the nature of the flow both at the given angle of incidence, and at maximum lift.

In Fig. 5, therefore, the total lift, and the separate lifts on the wing and the flap, for the configuration with the flap deflected 30°, are compared with values calculated for inviscid

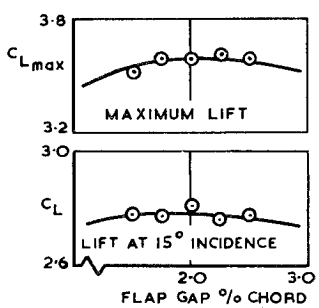

Fig. 4 Experimental effect of flap gap. Flap deflection 10°, slatted leading edge.

† With this definition of gap it should be noted that, when the flap is set at 10° deflection, the minimum distance between the wing trailing edge and the flap is larger than the defined gap, i.e. when the nominal gap is 2% chord the minimum distance is 3% chord.

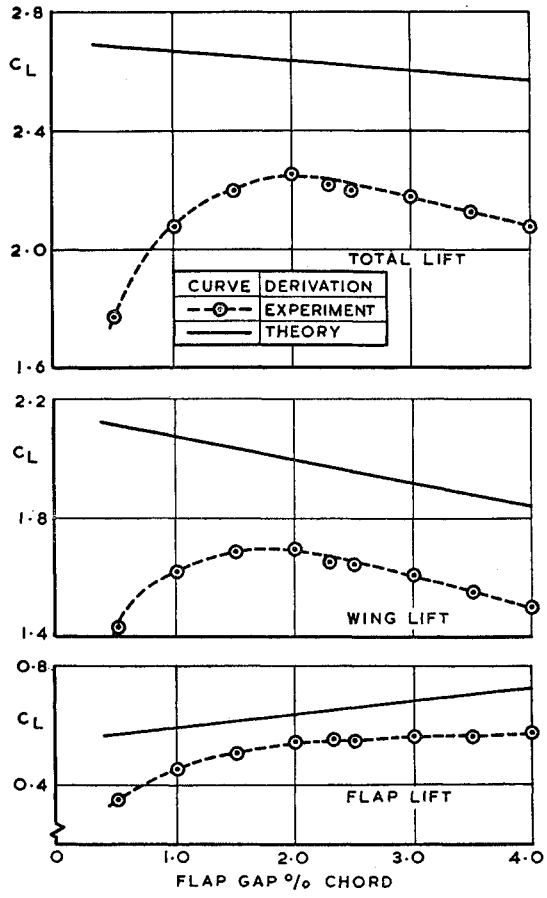

Fig. 5 Comparison of experimental and theoretical effect of gap. Flap deflection 30°, drooped leading edge.

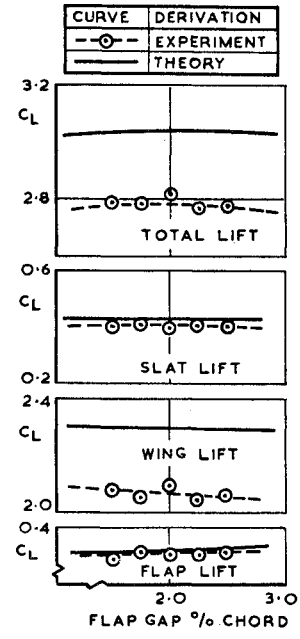

Fig. 6 Comparison of experimental and theoretical effect of gap. Flap deflection 10°, slatted leading edge.

flow, at the same angle of incidence. Although the experimental values follow the inviscid trends with variation of gap for gap settings greater than that which gives the highest total lift, the curves of both wing and flap lift depart from the inviscid trends for gap settings less than the optimum value. As the optimum gap indicated by the calculations for inviscid flow is zero, the existence of a non-zero optimum in the real flow must be attributed to viscous effects. Moreover, since the optimum gap marks the lower limit of the range of gap settings for which the measured values follow the inviscid trends, it must have resulted from some change in the nature of the effect of the viscous flows on the lift of the wing and flap.

The results of a similar comparison for the configuration with the flap deflected 10°, Fig. 6, show a somewhat different pattern with changes of flap gap. The variation of the lift on all the components of the multiple aerofoil is small, with no marked departure from the inviscid trends. The total lift, as calculated for inviscid flow does, however, indicate a highest value at a gap setting close to the experimentally determined optimum gap. For this configuration, therefore, the existence of an optimum gap appears to be attributable to inviscid effects, with viscous effects not showing a significant variation over the range of gap settings considered.

In order to reconcile these two apparently differing mechanisms for the occurrence of an optimum gap the velocity distributions through the viscous layer, measured at the trailing edge of the wing and in the flow over the flap, will be considered. Figure 7 shows some distributions‡ for a range of flap gaps. From the measurements at the position of the wing trailing edge, it can be seen that, for the range of gap settings for which the measured variation of lift with gap follows that calculated for inviscid flow, the boundary layer on the flap upper surface and that on the wing lower surface are separated by a region of freestream flow with full total head. The measurements at a gap of 2% chord suggest that this gap represents the limit of the separateness of the two boundary layers. At a gap of 0.5% chord, the two boundary layers are well mixed, with no freestream flow in the gap. The velocity distributions in the flow over the flap, for the various gap settings, reflect the differences found in the flow at the wing trailing edge. For the smallest gap, the wake from the wing and the boundary layer on the flap rapidly become completely mixed, and the flow soon separates from the flap

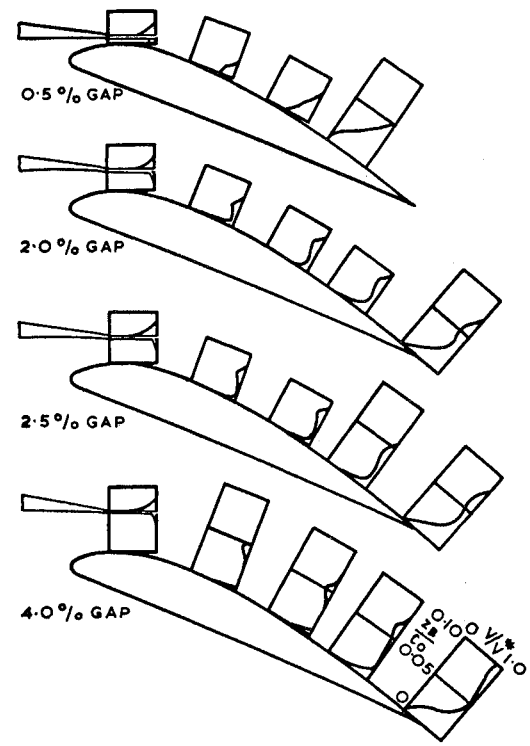

Fig. 7 Velocity distributions in flow over flap behind drooped leading edge.

‡ The figures show V/V^*, where V is the local flow velocity, and V^* is a calculated velocity corresponding to the local static pressure. V^* may vary across the viscous layer.

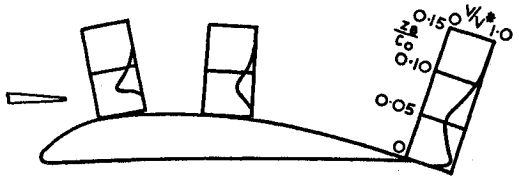

Fig. 8 Velocity distributions in flow over flap behind slatted leading edge.

surface. In contrast, the flow over the flap for gaps of 2% chord and greater is characterized by weak interference, with the flap boundary layer and wing wake retaining their separate identities almost to the flap trailing edge. Figure 8 shows velocity distributions measured for the flap deflection of 10° and the slatted leading edge; these distributions are typical for the range of flap gaps tested at this flap deflection. The smaller flap deflection, and the smoother shape of the wing lower surface (Fig. 2), have resulted in the flap boundary layer and the wake from the wing and slat being separated by a large region of freestream flow near to the wing trailing edge. Further, there is little subsequent interference between the wake from the wing and slat and the flap boundary layer, in the flow above the flap. It is the slat wake, incidentally, which results in the long 'tail' of the upper wake component.

It thus appears that while the flap boundary layer, and the boundary layer on the wing lower surface, remain separate, the forces on the wing and flap will vary with gap in a manner similar to that predicted by inviscid theory. If inviscid theory predicts an optimum gap in the range for which the boundary layers are separate, the optimum in the real flow will be close to this predicted value. If, however, the flap boundary layer and wing boundary layer meet at a gap greater than that for which inviscid theory would predict an optimum, the meeting of the boundary layers will define the limit of the similarity in behavior between the real flow and the inviscid flow. Any subsequent reduction of the gap setting will result in freestream flow not being present in the flow through the gap. As a consequence, the circulation around the wing will be reduced, and the strong mixing of the viscous flow over the flap will cause premature separation of the flow, so reducing the contribution of the flap to the total lift. Under these circumstances, therefore, the optimum gap is at, or very near to, the smallest gap at which the boundary layer on the flap and the boundary layer on the wing lower surface are just separate.

Flow around the Wing and Slat

Following the lines of the previous analysis, consideration is first made of the variation of the maximum lift coefficient, and that of the lift at constant angle of incidence, with slat gap. Figure 9 shows that the two curves are dissimilar, in contrast to those for the effect of flap gap. While there is a well defined optimum for the maximum lift coefficient, no such optimum occurs in the curve for the lift at a constant angle of incidence.

Although analysis of the lift at a constant angle of incidence cannot be expected to yield information as directly relevant to the maximum lift as for the flap case, it is still useful to compare the theoretical and experimental effect of variation of slat gap on the total lift, and the separate lifts on the components of the multiple aerofoil. Figure 10 shows that the experimental lift coefficients follow the inviscid trends quite closely. The dissimilarity at large gaps in the trends of the theoretical and experimental curves for total lift can be seen to be attributable to a similar departure for the wing lift. This occurs because the chosen angle of incidence, 15°, while being some 7° below the angle of incidence for the stall for the optimum gap, is only 3° below the stall for the largest

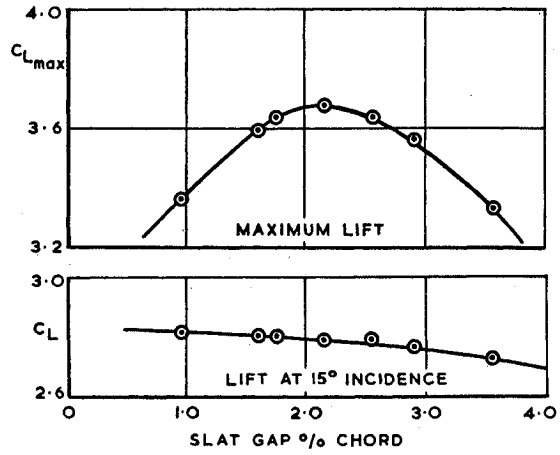

Fig. 9 Experimental effect of slat gap. Slat deflection 28°.

gap, and the lift curve slope has been reduced due to the incipient stall. If this region is therefore considered as unrepresentative it can be seen that the experimental lift coefficients follow the inviscid trends for the complete range of slat gaps.

Figure 11 shows velocity distributions through the viscous layer above the wing for three slat gaps. The flow is very similar for all three gaps, being characterized by strong mixing between the slat wake and the wing boundary layer, so that near to the wing trailing edge the two layers are almost completely merged. Variation of the slat gap has not resulted in an obvious change in the development of the interaction between the slat wake and the wing boundary layer, as was the case for the flow over the flap with variation of flap gap.

Figure 10 does suggest that, as the slat gap was reduced, the

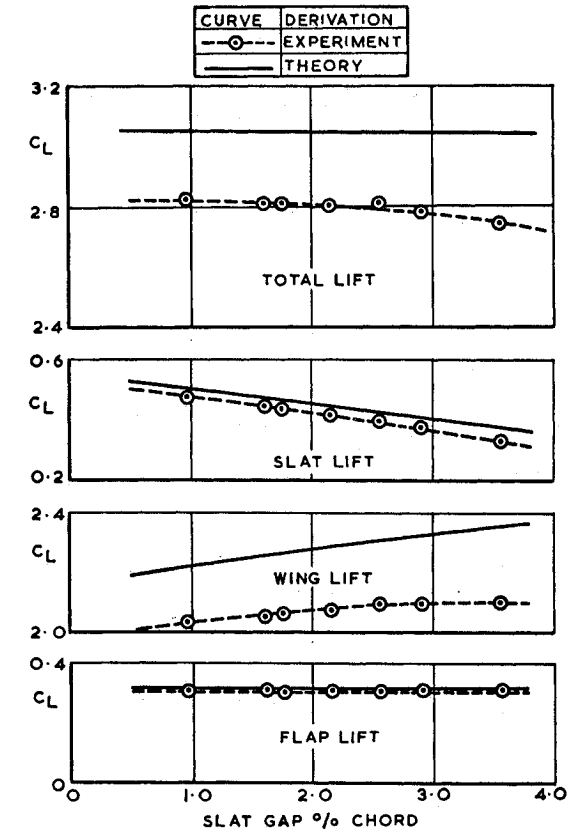

Fig. 10 Comparison of experimental and theoretical effect of gap. Slat deflection 28°, flap deflection 10°.

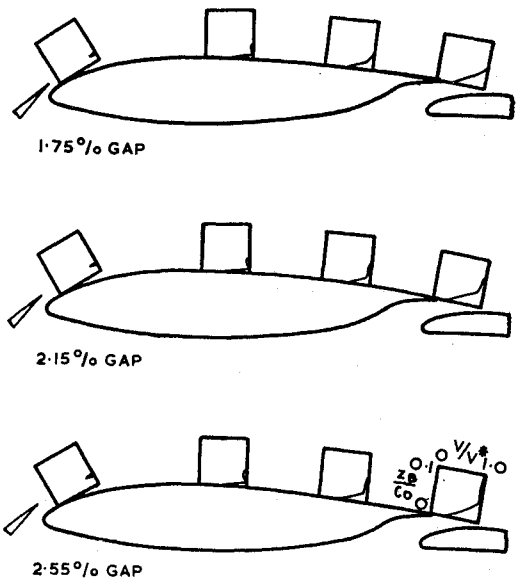

Fig. 11 Velocity distributions in flow over wing behind slatted leading edge.

total lift remained almost constant, but the lift contributed by the wing decreased. Hence, in the absence of any viscous interaction, and if the wing is assumed to stall at a given lift, it might be expected that the stalling incidence, and the total lift at the stall, would increase with decreasing gap. This effect is found in the experimental results for gap settings greater than the optimum, but for smaller gaps the trend reverses. This must be the result of a viscous interaction, and the manner in which this interaction affects the flow in the viscous layer can be determined from the detailed profile of the layer. The most marked effect occurs in the part of the layer adjacent to the wing surface, and to illustrate this values of the skin friction on the wing surface, measured by the razor-blade technique,[6] are shown in Fig. 12 for three values of the slat gap. It can be seen that, as the slat approaches the wing, the interference between its wake and the wing boundary layer results in the wing boundary layer being brought closer

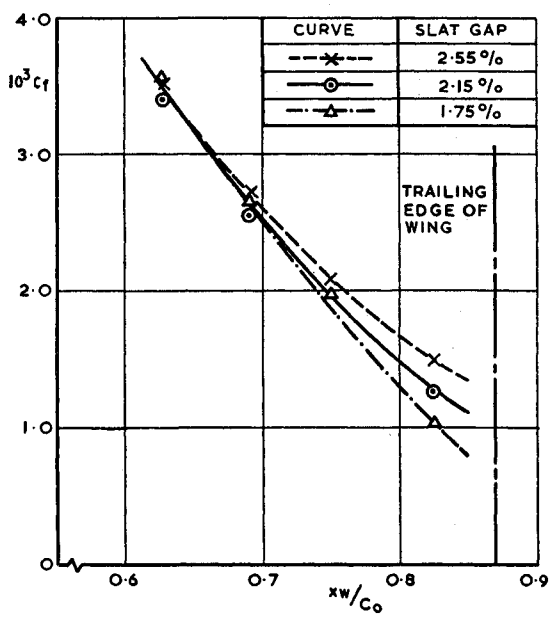

Fig. 12 Skin friction distribution on wing behind slatted leading edge.

to separation. Thus, although for the small values of the slat gap the wing contribution to the total lift is smallest, the viscous interference results in premature separation of the flow on the wing, and a reduced maximum lift coefficient. The optimum slat gap therefore results from a balance of the inviscid benefits of reducing the gap and of the adverse effects of the viscous interaction.

Prediction of the Optimum Position of the Slat and Flap, and of the Corresponding Flow

The analysis given previously suggested that the optimum position of the flap could be obtained from considerations of the effect of flap position on the inviscid lift, and of the meeting of the boundary layers on the wing lower surface and flap upper surface. The thicknesses of these boundary layers should be calculated for the pressure distributions corresponding to the real flow, and the calculation for the boundary layer on the wing lower surface should include the effect of the separation and reattachment of the flow which occurs on the lower surface of the wing. The subsequent discussions lead to the conclusion that the calculation of the optimum slat position will require a complete knowledge of the real flow around the wing and slat, to determine the interaction between the viscous interference, and the effect of the slat position on the inviscid lift.

A method of predicting the real flow around a wing with high-lift devices will need calculations of 1) the inviscid pressure distribution around the multiple aerofoil, 2) the development of the viscous layers around the multiple aerofoil, and 3) the incorporation of the viscous layers into the inviscid calculations. The method used for the calculation of the inviscid pressure distribution[4] is quite satisfactory, and no further development is currently considered necessary.

Calculations for the development of the boundary layer on the most upstream component of the multiple aerofoil can use existing boundary-layer calculation methods. However, the calculation of the development of the viscous layer for the downstream component is complicated by the fact that the boundary layer on the upper surface develops under the wake from the upstream component. Work on a calculation method for the simultaneous development of a wake and a boundary layer is proceeding at RAE, and the results of an initial investigation, using an integral method, will be published shortly.

However, as the flow for the optimum flap position has been defined as one in which there is only weak interference between the wing wake and the flap boundary layer, it is of interest to ascertain the effect of ignoring the interference completely, and of using existing calculation methods for the separate development of the boundary layer and wake. Figure 13 compares experimental values of the displacement and momentum thicknesses, for the complete viscous layer above the flap, with values calculated in this way. The method used was an extension of Head's entrainment method[7] for turbulent boundary layers, due to Green,[8] with experimentally determined pressure distributions, and starting from experimental measurements of the displacement and momentum thickness. For the flap deflection of 30° (Fig. 13a), quite reasonable agreement is achieved up to the position at which the viscous flow separates from the flap. Similar close agreement is achieved when the flap deflection is reduced to 10°, and the plain leading edge is fitted (Fig. 13b). However, when this leading edge is replaced by the slatted leading edge (Fig. 13c), the calculated values do not agree with the experimental values. This is because some empirical constants, used in the calculation of the growth of the wake, were derived from experiments in which the velocity distribution through the wake was of Gaussian form, whereas the presence of the slat wake makes the velocity distribution in the upper half of the wake non-Gaussian.

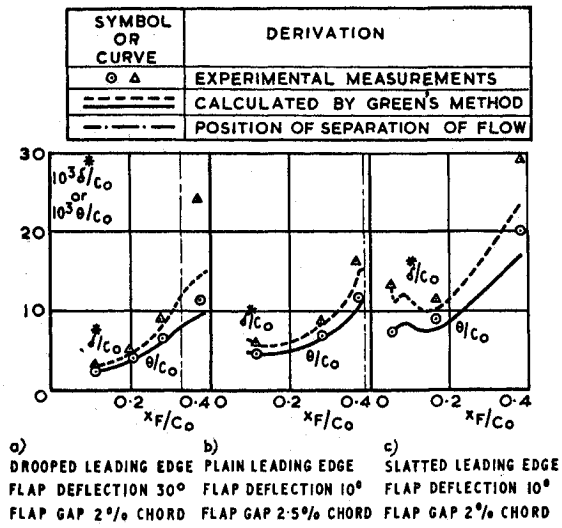

Fig. 13 Comparison of theoretical and experimental growth of viscous layer over flap.

Figure 14 shows a similar comparison for the flow over the wing behind the slatted leading edge. Quite surprisingly, in view of the strong mixing which is occurring between the slat wake and the wing boundary layer, the disagreement between measured and calculated values is no worse than for the flow above the flap, where the interference is weak. It may thus be concluded that for the configurations considered in these figures, the external influences in the form of the pressure gradients predominate over the influence of the internal turbulence structure. The measure of agreement shown does not, however, obviate the need for the general calculation method discussed earlier.

The growth of the boundary layer on the most upstream component of the multiple aerofoil may be included in a calculation of the inviscid pressure distribution in the classical manner, by adding to the aerofoil contour the displacement thickness of the boundary layer. However, for the downstream components, the wake from the upstream components again presents an additional complication. Only, perhaps, when the wake and boundary layer are well mixed, as at the trailing edge of the wing with a slatted leading edge, can the displacement thickness concept be used. When the wake is nominally separate from the boundary layer, the presence of this shear layer must affect the lift of the component below it. Work is currently in progress to estimate the magnitude of this effect, using the measured wake development over the flap, prior to consideration of a method of incorporating the development of the wake into a calculation method.

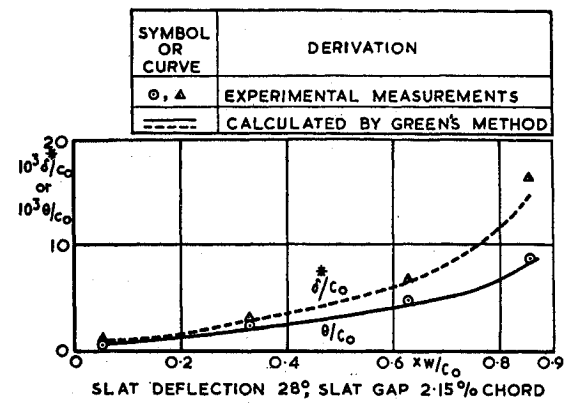

Fig. 14 Comparison of theoretical and experimental growth of viscous layer over wing.

Conclusions

Having defined the nature of the two-dimensional flow around the wing with high-lift devices, it is possible to suggest the manner in which the characteristics of the high-lift system are likely to be affected by changes of Reynolds number, and how this work might be extended to the three-dimensional flow on a sweptback wing.

Considering first the wing and flap, the effect of changes of Reynolds number will depend on whether the optimum position of the flap is determined by inviscid or viscous effects. For the situation such as was discussed above for the small flap deflection, where the optimum flap gap is very close to the inviscid optimum, increase of Reynolds number will increase the maximum lift coefficient in the conventional manner, but the optimum flap position is unlikely to be affected. In contrast, when the optimum gap is close to the gap at which the boundary layer on the wing lower surface, and that on the flap upper surface meet, increase of Reynolds number should result in these boundary layers becoming thinner, and so the size of the gap at which they meet will be reduced, with a consequent increase in the maximum lift. Such an effect was, in fact, measured experimentally some years ago in some NACA tests.[9] The effect of changes of Reynolds number on the optimum slat position should again be to allow the gap to be reduced as Reynolds number is increased, since the thickness of both the wing boundary layer and the slat wake should decrease with increasing Reynolds number.

The nature of the flow described here should be reproduced on a sweptback wing for the region of the span for which 'sheared flow' conditions exist. Away from this region, center or tip effects predominate, and these will lead to modifications to the chordwise pressure distributions, and to the development of the boundary layers and wakes. Measurements, similar to those described here, are to be made of the flow around a swept-back wing with a slat and flap, for a range of spanwise positions. It is intended that the analysis will, initially, follow the lines considered in this paper. Further, it should be possible to synthesize a calculation method from basic elements similar to those described here, using, it is hoped, extensions of methods currently under development.

References

[1] Young, A. D., "The Aerodynamic Characteristics of Flaps," R and M 2622, 1947.

[2] *USAF Stability and Control Handbook*, US Air Force Flight Dynamics Laboratory, Wright-Patterson Air Force Base, Ohio.

[3] Foster, D. N., "Note on Methods of Calculating the Pressure Distribution over the Surface of Two-Dimensional Cambered Wings," TR 67095, 1967, Royal Aircraft Establishment, Farnborough, Hampshire, England.

[4] Hess, J. L. and Smith, A. M. O., "Calculation of Potential Flow about Arbitrary Bodies," *Progress in Aeronautical Sciences*, Vol. 8, No. 1, Pergamon Press, London, 1967, p. 138.

[5] Foster, D. N. and Lawford, J. A., "Experimental Attempts to Obtain Uniform Loading over Two-Dimensional High-Lift Wings," TR 68283, 1968, Royal Aircraft Establishment, Farnborough, Hampshire, England.

[6] East, L. F., "Measurements of Skin Friction at Low Subsonic Speeds by the Razor-Blade Technique," R and M 3525, 1966, Aeronautical Research Council, London, England.

[7] Head, M. R., "Entrainment in the Turbulent Boundary Layer," R and M 3152, 1958, Aeronautical Research Council, London, England.

[8] Green, J. E., "Head's Method in Compressible Flow," RAE TR, to be published.

[9] Racisz, S. F., "Investigation of NACA 65(112)A111 (approx.) Airfoil with 0.35 Chord Slotted Flap at Reynolds Numbers up to 25 Million," TN 1463, 1947, NACA.